Supporting Information

Wei et al. 10.1073/pnas.1013012108

SI Materials and Methods

RT-PCR, Plasmid Construction, and Lentivirus Production. Prokaryotic expressing plasmids were constructed using the Gateway cloning system. Mission Lentiviral ShRNA and nontarget controls were commercially obtained and lentiviral particles were produced as suggested (Sigma-Aldrich). For specific knockdown of Srx or Prx, a set of four ShRNA constructs for each gene targeting to different mRNA regions was examined and evaluated. The ShRNA construct that has the highest knockdown efficiency, which also targets the coding region, was used for further study. The Lenti-X expression system (Clontech) was used for stable overexpression of Srx, and the Gateway lentiviral expression system (Invitrogen) was used for ovexpression of Prx IV. The infectious lentiviral particles were produced using commercial packaging systems (Clontech and Invitrogen) in HEK293T cells according to the manufacturers' suggested protocols.

Cell Culture, Transient Transfection, Lentivirus Infection, Flow Cytometry, and Gelatin Zymography. HEK293T human embryonic kidney cells and cell lines from human lung normal epithelium or lung primary tumor/metastasis were commercially obtained from the National Cancer Institute repository or ATCC. All cells were cultured in the provider's suggested conditions. Three immortalized lung normal epithelial cell lines were used, including BEAS-2B (immortalized by SV40 T antigen), NL20 (immortalized by SV40 T antigen), and Nuli-1 (immortalized by HPV-E6/7 and hTERT). Two cell lines derived from lung small cell carcinoma were used including NCI-H69 and NCI-H82 cells. Three cell lines from lung squamous cell carcinoma were used, including NCI-H520 (derived from primary tumor), NCI-H226, and SK-Mes-1 (both were derived from pleural effusion). Three cell lines from lung adenocarcinoma were used, including A549 (derived from primary tumor), NCI-H2030 (derived from lymph node metastasis), and NCI-H2122 (derived from pleural effusion). HEK293T and JB6P$^+$ transformation-sensitive mouse epidermal cells were cultured in standard conditions and transfection was performed using FuGENE 6. A modified XTT assay (Roche) was used to examine cell growth and proliferation. Lentivirus infection was performed using standard protocols with polybrene. A549 cells were stably transfected by infection of lentiviral particles expressing an empty vector (ShV), a nontarget ShRNA (ShNT), or an ShRNA construct containing a hairpin structure-specific target to human Srx coding region (ShSrx). The cell-cycle phase determination kit (Cayman Chemical) and flow cytometer (BD Bioscience) were used for cell-cycle analysis. For gelatin zymography, cells were cultured in serum-free medium and the concentrated culture medium was separated on native SDS/PAGE gel containing 0.1% gelatin. The zymogram was performed following the manufacturer's suggested protocols (Invitrogen).

Western Blotting, Immunoprecipitation (IP), and Phosphokinase Profiling. Western blotting and IP were performed using RIPA lysis buffer (Santa Cruz) with a standard protocol. According to the affinity of the antibodies and the protein molecular weight, membranes were cut and stripped for multiple Western blots to minimize the variation. In Fig. 6*B*, all cells were cultured in T75 flasks, cells were collected by trypsinization, and cell numbers were counted in a Coulter cell counter. Cells were then lysed in RIPA buffer at the concentration of 2×10^7 cells/mL. All primary antibodies were commercially obtained, including goat anti-Srx, rabbit anti-Prx II, mouse anti-Prx III, mouse anti-c-Myc, rabbit anti-c-Jun, and mouse anti-Akt1 (Santa Cruz); rabbit anti-Srx (Proteintech); mouse anti-Prx IV (Abfrontier); rabbit anti-Prx I (Abcam); mouse anti–β-actin and mouse anti-Flag (Sigma-Aldrich); mouse anti-MEK1 and mouse anti-KSR1 (BD Bioscience); and rabbit anti-p-PP2A (R&D Systems); and all other antibodies were obtained from Cell Signaling. For phosphokinase profiling, cells were serum starved for 24 h and then stimulated with serum-containing medium plus 10 ng/mL TPA for 30 min. Cells were then lysed in RIPA buffer and the proteome profiler human phosphokinase profiling and MAPK profiling were performed following the manufacturer's suggested protocols (R&D Systems).

Anchorage-Independent Growth, Wound Healing, and Transwell Matrigel Invasion Assay. Cells were cultured in soft agar and colonies were examined under the microscope with or without neutral red staining (Sigma-Aldrich) or scanned with a Gelcount Scanner (Oxford Optronix). For the wound-healing assay, cells were seeded in 24-well plates at a density of 5×10^4 cells per well for rapid confluence. The wounds were made by scratching with a sterile 200-μL pipette tip. Floating cells were removed by rinsing three times with PBS. Images of cell migration at different time points were recorded using the microscopic image station. For transwell matrigel invasion assay, cells were cultured in a 24-well transwell invasion chamber and the invasion assays were performed following the manufacturer's suggested protocols (BD Bioscience). Invaded cells were stained by Diff-Quik staining and cell numbers were counted by Image J software.

Reverse-Phase Liquid Chromatography–Mass Spectrometry (RPLC-MS), Recombinant Protein Purification, and Surface Plasmon Resonance (SPR). HEK293T, A549, or JB6P$^+$ cells were transiently transfected with plasmid expressing Flag-Srx or empty vector (control). Anti-Flag IPs for mass spectrometry were performed. To increase the specificity and reliability of the protein identification, three strategies for RPLC-MS were used. First, the IP eluates from either control cells or Flag-Srx–transfected cells were concentrated and analyzed directly by RPLC-MS. Second, the concentrated IP eluates were separated by SDS/PAGE and stained by silver staining, and the identities of the differential bands were then determined by MS. Third, three cell lines (HEK293T, JB6, and A549) were used for independent experiments. These cells vary in the levels of endogenous Srx expression, from none (HEK293T) to low (JB6P$^+$) or medium (A549) levels. The transfection efficiency is also different in these cells, with the highest Flag-Srx expression in HEK293T cells and the lowest in JB6P$^+$ cells. The IP eluates were concentrated by lyophilization and then either subjected to direct digestion or separated by SDS/PAGE and visualized by silver staining (Invitrogen). The differential bands in Flag-Srx IP were excavated and destained in the destaining solution (50% acetonitrile, 25 mM NH_4HCO_3, pH 8.4). Samples were lyophilized again and digested overnight at 37 °C in the digestion buffer (25 mM NH_4HCO_3, pH 8.4, containing 20 ng/μL trypsin). The reaction was then treated with the extraction buffer (70% acetonitrile and 5% formic acid). The extracted peptide solution was lyophilized and reconstituted in 0.1% formic acid before being subjected to RPLC using the C-18 nanoRPLC column and the Agilent 1100 nanoLC system, which was coupled to a linear ion-trap mass spectrometer (LTQ). Peptides were eluted using a stepwise gradient of mobile phase A (0.1% formic acid in water) and B (0.1% formic acid in acetonitrile). The tandem mass

spectra were searched against the UniProt human (HEK293T and A549 cells) or mouse (JB6 cells) proteomic database using SEQUEST software.

The prokaryotic expression clones were transformed into *E. coli* and proteins were purified by immobilized metal affinity chromatography in an AKTA Purifier workstation (GE Healthcare). The SPR assay was performed with assay buffer containing 20 mM Hepes (pH 7.5), 150 mM NaCl, 5 mM DTT, 100 μM TCEP, 0.005% Tween20, 0.1% BSA, and 5 mg/mL dextran. The purified Prxs and control MBP were amine coupled to a Biacore sensor chip and series of Srx concentrations were injected over the chip surface. Complex formation was monitored in a Biacore 3000 instrument and the binding kinetics were analyzed using the computer software.

Mouse Xenografts and Lung Metastasis. All mouse experiments were performed at the National Cancer Institute (Frederick, MD) animal facility according to the rules and regulations of the Animal Care and Use Committee and the guidelines of the Animal Welfare Act. A total of 80 SCID/NCr female mice (BALB/C background) at 6 wk of age were randomly separated into eight groups ($n = 10$ in each group). For s.c. injection, each mouse was injected with 5×10^6 cells to the back and tumor volume was measured every other day using a caliber. Mice were killed ∼40 d after injection as the tumor volume was ∼1,000 mm^3. Tumors were extracted from the mouse skin and net tumor weight was measured. For lung metastasis, each mouse was injected with 2×10^5 cells through the tail vein. Thirteen weeks later (3 mo) mice were anesthetized with Avertin and lungs were perfused with PBS for counting visible tumor nodules (with a diameter ≥1 mm). The paraformaldehyde-fixed lungs were further processed and H&E staining was performed using a standard histological protocol.

Statistical Analysis. Quantitative data were presented as means ± SD ($\bar{x} \pm$ SD). For calculation of the P value, a two-tailed, unpaired Student's t test or a paired t test was used as specified.

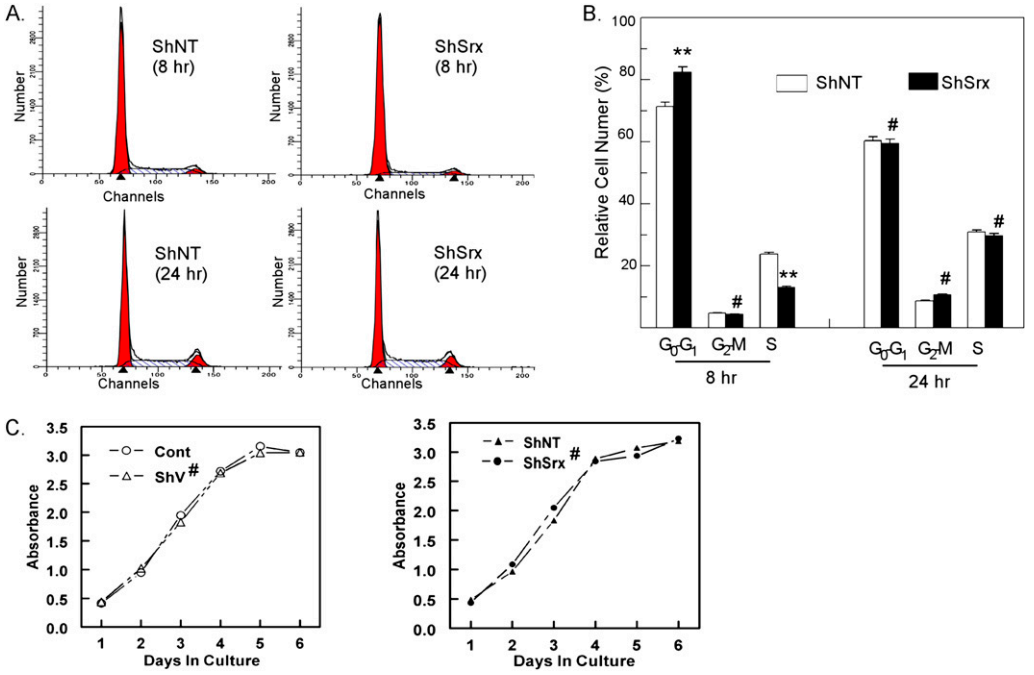

Fig. S1. Knockdown of Srx in A549 cells briefly delays serum-induced cell-cycle progression but does not inhibit cell growth under adherent conditions. (*A* and *B*) Cell-cycle analysis using propidium iodide and flow cytometry. A549 cells were stably transfected by infection of lentiviral particles expressing an empty vector (ShV), a nontarget ShRNA (ShNT), or an ShRNA construct containing a hairpin structure-specific target to the Srx coding region (ShSrx). Cells were serum starved for 24 h before being replenished with serum-containing medium and harvested 8 or 24 h later. Data are presented as means ± SD ($n = 3$). Compared with the control, $^{\#}P > 0.05$, $^{**}P < 0.01$ (t test). (*C*) A549 cells were cultured in 96-well plates and cell proliferation was measured by XTT assay. Data are presented as means ± SD ($n = 6$). Compared with the control or ShNT, $^{\#}P > 0.05$ (t test).

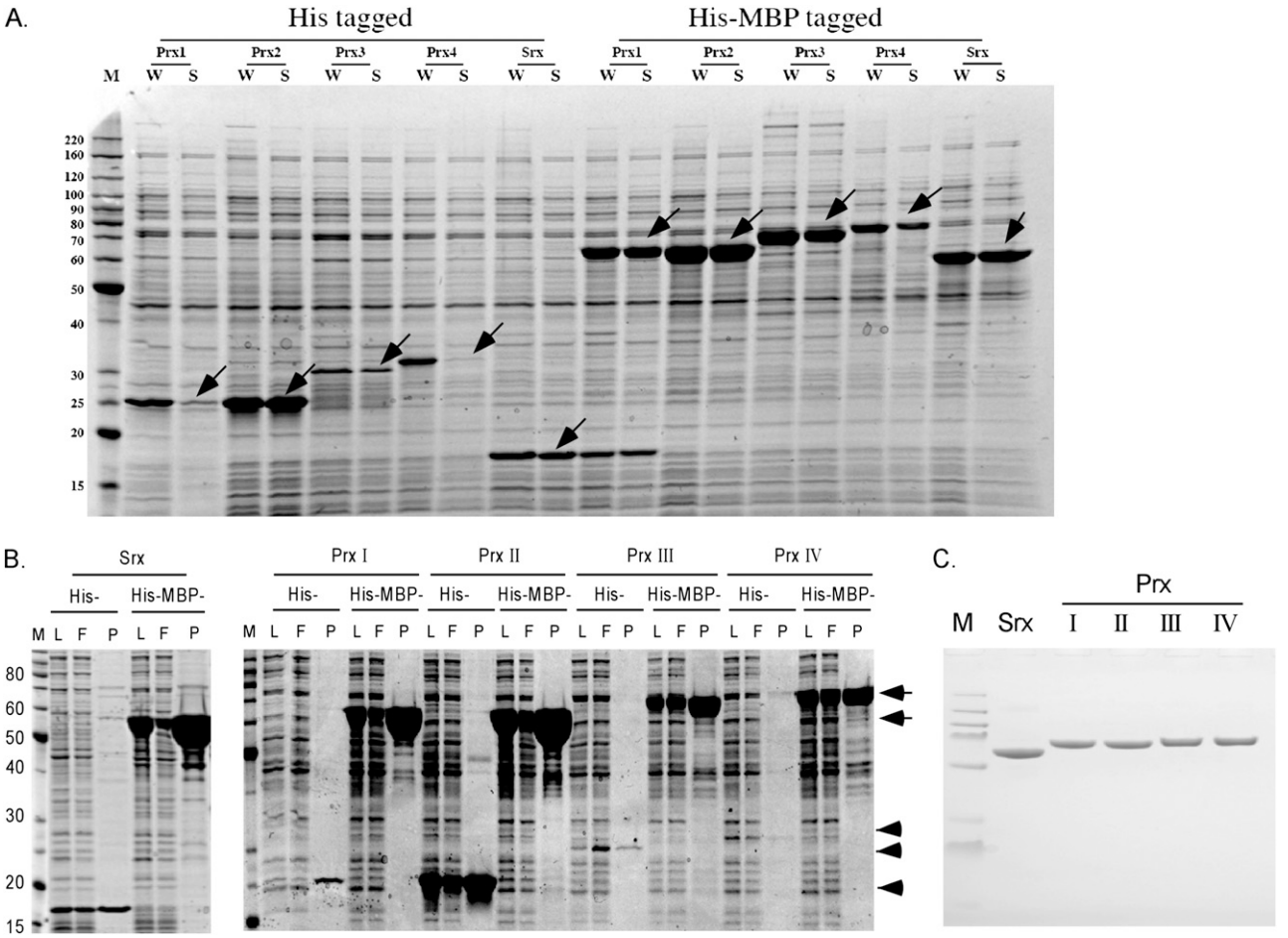

Fig. S2. Purification of recombinant Srx and Prxs. (*A*) Assessment of the solubility of recombinant Srx and Prxs expressed in *E. coli.* M, protein standard in kilodaltons; W, total bacterial lysates; S, supernatant of bacterial lysates. Proteins extracted from a small preparation were separated on a 10% gel by SDS/PAGE and stained with Coomassie blue. Arrows indicate the band of soluble recombinant Srx or Prxs with His or His-MBP tagged. (*B* and *C*) Tandem-affinity purification of recombinant Srx and Prxs from *E. coli.* L, total bacterial lysates; F, flow-through fraction from the nickel column; P, eluted fraction. Arrows indicate the position of Srx or Prxs. (*C*) The final purified proteins were stained by Coomassie blue.

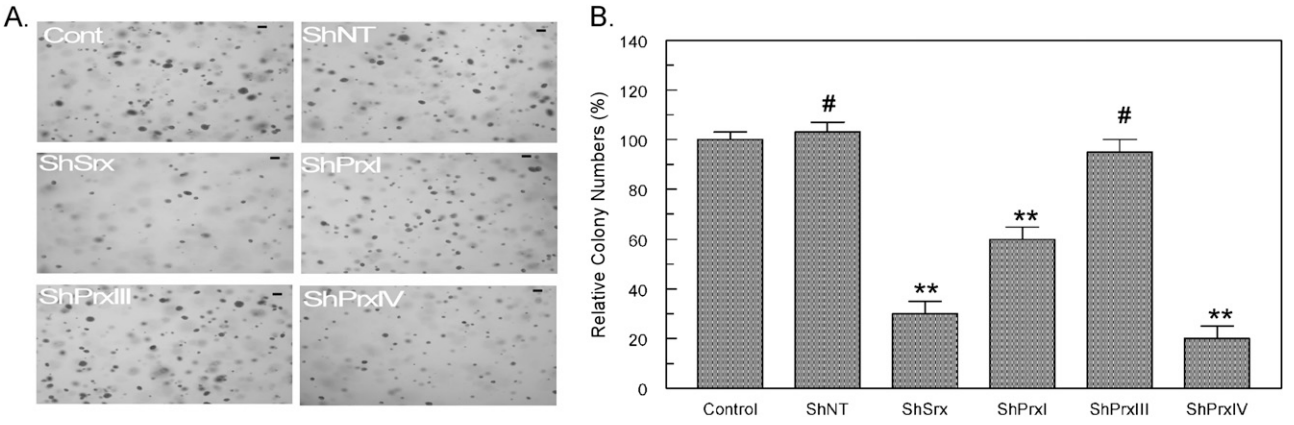

Fig. S3. Prx IV knockdown cells form fewer anchorage-independent colonies in soft agar. A549 cells were stably transfected by infection of lentiviral particles expressing a nontarget ShRNA (ShNT) or an ShRNA construct containing a hairpin structure-specific target to the coding region of Srx (ShSrx), PrxI (ShPrxI), Prx II (ShPrxII), PrxIII (ShPrxIII), or PrxIV (ShPrxIV). Representative images are shown and colonies with diameter >100 μm (scale bar in *A*) were counted. Data are presented as means ± SD ($n = 6$). Compared with the control parental cells, $^{\#}P > 0.05$, $^{**}P < 0.01$ (*t* test).

A.

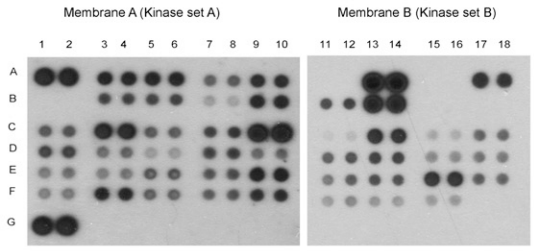

B.

Membrane/Coordinate	Target/Control	Phosphorylation Site
A - A1, A2	Positive Control	—
A - A3, A4	p38α	T180/Y182
A - A5, A6	ERK1/2	T202/Y204, T185/Y187
A - A7, A8	JNK pan	T183/Y185, T221/Y223
A - A9, A10	GSK-3α/β	S21/S9
B - A13, A14	p53	S392
B - A17, A18	Positive Control	—
A - B3, B4	MEK1/2	S218/S222, S222/S226
A - B5, B6	MSK1/2	S376/S360
A - B7, B8	AMPKα1	T174
A - B9, B10	Akt	S473
B - B11, B12	Akt	T308
B - B13, B14	p53	S46
A - C1, C2	TOR	S2448
A - C3, C4	CREB	S133
A - C5, C6	HSP27	S78/S82
A - C7, C8	AMPKα2	T172
A - C9, C10	β-Catenin	—
B - C11, C12	p70 S6 Kinase	T389
B - C13, C14	p53	S15
B - C15, C16	p27	T198
B - C17, C18	Paxillin	Y118
A - D1, D2	Src	Y419
A - D3, D4	Lyn	Y397
A - D5, D6	Lck	Y394
A - D7, D8	STAT2	Y689
A - D9, D10	STAT5a	Y699
B - D11, D12	p70 S6 Kinase	T421/S424
B - D13, D14	RSK1/2/3	S380
B - D15, D16	p27	T157
B - D17, D18	PLCγ-1	Y783
A - E1, E2	Fyn	Y420
A - E3, E4	Yes	Y426
A - E5, E6	Fgr	Y412
A - E7, E8	STAT3	Y705
A - E9, E10	STAT5b	Y699
B - E11, E12	p70 S6 Kinase	T229
B - E13, E14	RSK1/2	S221
B - E15, E16	c-Jun	S63
B - E17, E18	Pyk2	Y402
A - F1, F2	Hck	Y411
A - F3, F4	Chk-2	T68
A - F5, F6	FAK	Y397
A - F7, F8	STAT6	Y641
A - F9, F10	STAT5a/b	Y699
B - F11, F12	STAT1	Y701
B - F13, F14	STAT4	Y693
B - F15, F16	eNOS	S1177
B - F17, F18	PBS (Negative Control)	—
A - G1, G2	Positive Control	—
A - G5, G6	PBS (Negative Control)	—

C.

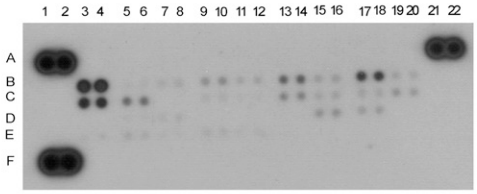

D.

Coordinate	Target/Control	Alternate Nomenclature	Phosphorylation Site Detected
A1, A2	Positive Control	Control (+)	—
A21, A22	Positive Control	Control (+)	—
B3, B4	ERK1	MAPK3, p44 MAPK	T202/Y204
B5, B6	JNK1	MAPK8, SAPK1γ	T183/Y185
B7, B8	JNK pan	—	T183/Y185, T221/Y223
B9, B10	p38γ	MAPK12, SAPK3, ERK6	T183/Y185
B11, B12	p38δ	MAPK13, SAPK4	T180/Y182
B13, B14	RSK1	MAPKAPK1α, RPS6KA1	S380
B15, B16	GSK-3α/β	GSK3A/GSK3B	S21/S9
B17, B18	Akt1	PKBα, RACα	S473
B19, B20	Akt2	PKBβ, RACβ	S474
C3, C4	ERK2	MAPK1, p42 MAPK	T185/Y187
C5, C6	JNK2	MAPK9, SAPK1α	T183/Y185
C9, C10	p38α	MAPK14, SAPK2A, CSBP1	T180/Y182
C11, C12	p38β	MAPK11, SAPK2B, p38-2	T180/Y182
C13, C14	RSK2	ISPK-1, RPS6KA3	S386
C15, C16	GSK-3β	GSK3B	S9
C17, C18	Akt3	PKBγ, RACγ	S472
C19, C20	Akt pan	—	S473, S474, S472
D5, D6	JNK3	MAPK10, SAPK1β	T221/Y223
D7, D8	MSK2	RSKβ, RPS6KA4	S360
D15, D16	HSP27	HSPB1, SRP27	S78/S82
D17, D18	p70 S6 Kinase	S6K1, p70α, RPS6KB1	T421/S424
E3, E4	Rabbit IgG	Control (-)	—
E5, E6	Mouse IgG_1	Control (-)	—
E7, E8	Mouse IgG_{2A}	Control (-)	—
E9, E10	Mouse IgG_{2B}	Control (-)	—
E11, E12	Goat IgG	Control (-)	—
E13, E14	PBS	Control (-)	—
F1, F2	Positive Control	Control (+)	—

Fig. S4. Antibodies and alignment of proteome profiler human phosphor-kinase array sets (*A* and *B*) and phosphor-MAPK array. (*A*) An example of an array showing the alignment of the spots. (*B*) Phospo-specific antibodies and their targeted phosphorylation sites used in the array. To identify particular kinases whose activation may mediate Srx signaling, the following criteria were used: (*i*) In ShNT cells, the level of phosphorylation was robustly induced upon stimulation compared with nonstimulated cells; (*ii*) in ShSrx cells upon stimulation, the induction of phosphorylation was significantly less than in ShNT cells; and (*iii*) in Srx cells under the same stimulation conditions, the level of phosphorylation was similar to or higher than that in ShNT cells. (*C*) An example of an array showing the alignment of the spots. (*D*) Phospo-specific antibodies and their targeted phosphorylation sites used in the array.

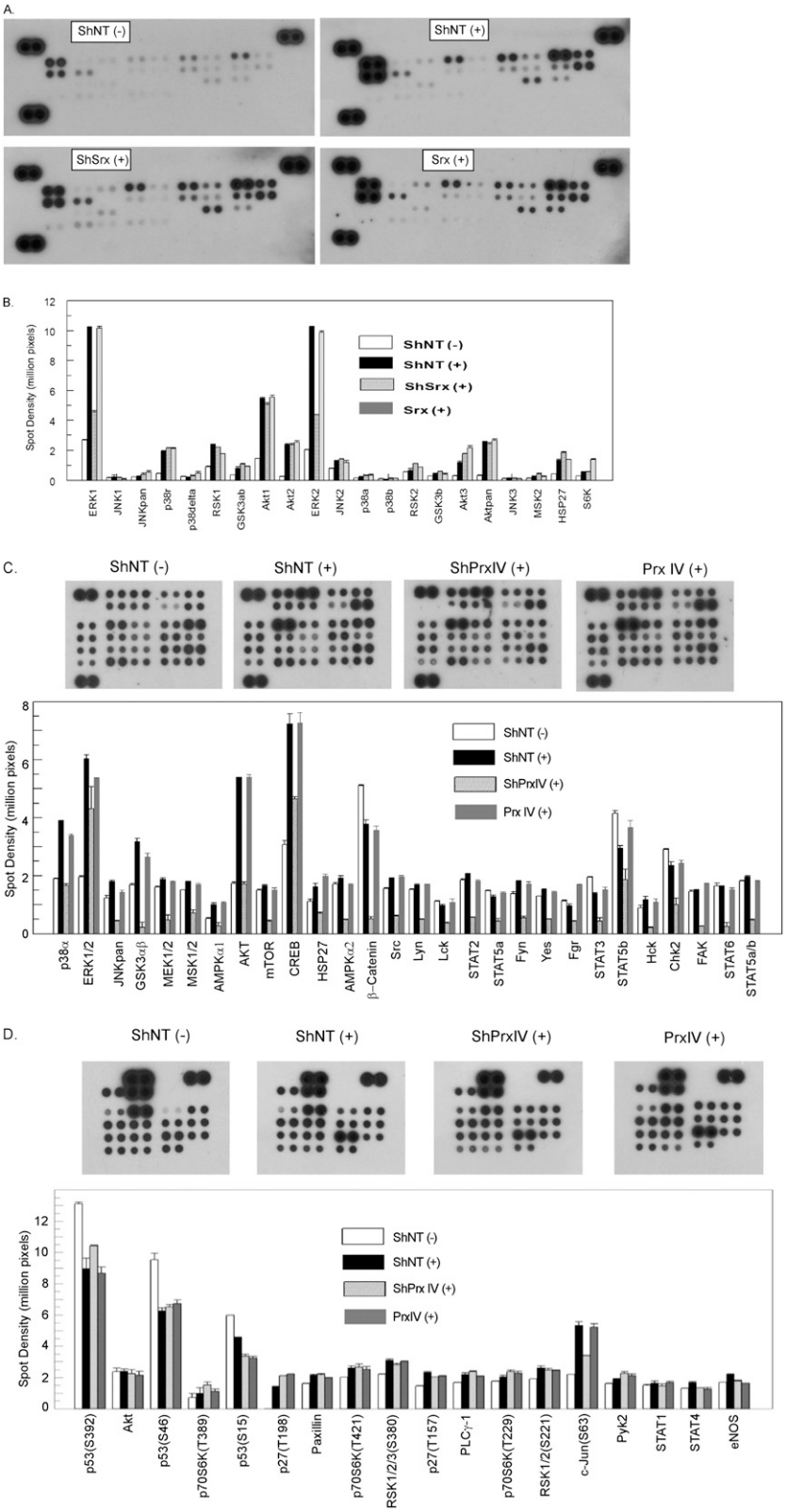

Fig. S5. Srx and Prx IV in phosphokinase signaling in A549 cells. (*A*) The proteome profiler human phosphor-MAPK array was performed using A549 cells as described in Fig. 3. A list of phosphor-specific antibodies and the array alignment are included in *SI Materials and Methods*. (*B*) Quantitation of spot intensity in *A*. Cells stably expressing ShNT, ShSrx, or Flag-Srx were serum starved for 24 h and stimulated with serum-containing medium. Cell lysates were harvested at the indicated times after stimulation. Proteome profiler human phosphokinase array sets A (*C*) and B (*D*) reveal PrxIV-related cell signaling changes in A549 cells. Cells were stably transfected by infection of lentiviral particles expressing an empty vector (ShV), a nontarget ShRNA (ShNT), or an ShRNA construct containing a hairpin structure-specific target to the Prx IV coding region (ShPrxIV). The array was performed as described in Fig. 3.

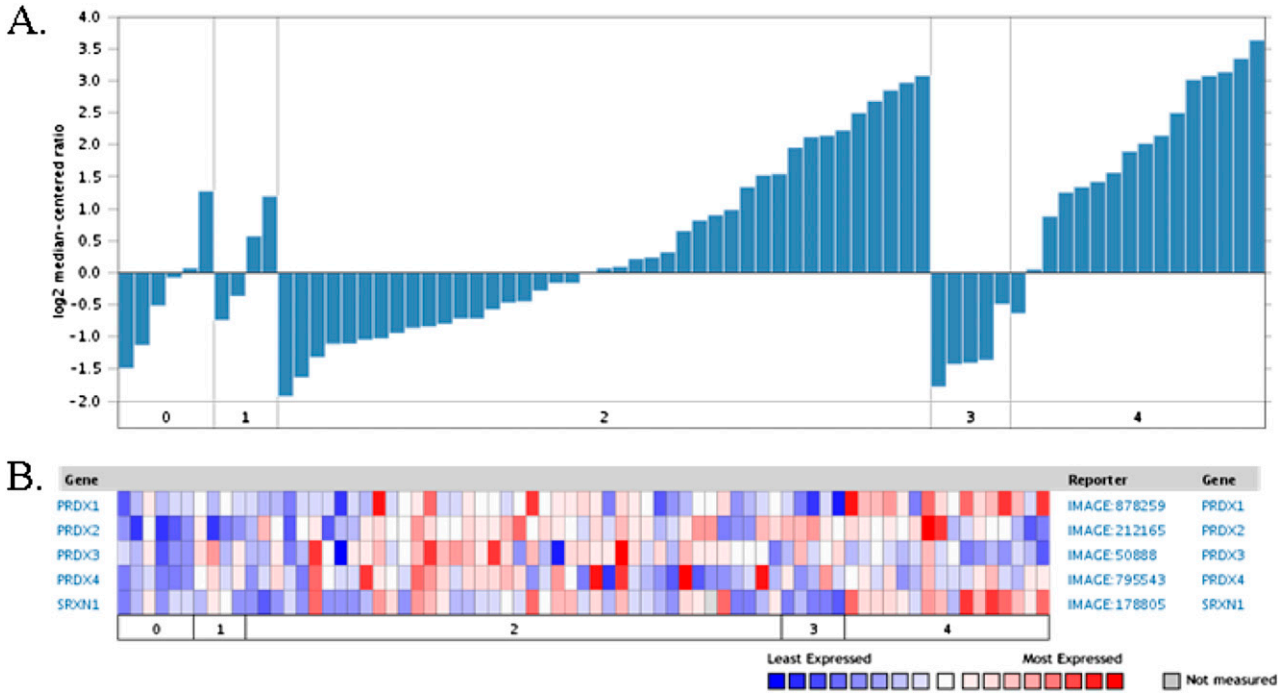

Fig. S6. Comparison of Prx I, Prx II, Prx III, Prx IV, and Srx mRNA expression in human lung normal and cancer tissues from the Oncomine database. (*A*) Srx mRNA expression in human lung normal and cancer tissues. (*B*) Heat map comparison of Srx and Prx expression in human normal and cancer tissues. Original data come from Garber et al. (1) and were analyzed with the Oncomine database (www.oncomine.com). Values in the assay: 0, normal lung (n = 6); 1, large cell lung carcinoma (n = 4); 2, lung adenocarcinoma (n = 42); 3, small cell lung carcinoma (n = 5); 4, squamous cell lung carcinoma (n = 16).

1. Garber ME, et al. (2001) Diversity of gene expression in adenocarcinoma of the lung. *Proc Natl Acad Sci USA* 98:13784–13789.

Table S1. Summary of histopathological features and patient information from sample cores on tissue microarray slides

	Normal		Nontumor disease		Cancer types and histopathological grading*								
					Squamous cell carcinoma				Adenocarcinoma				
	Normal	Cancer adjacent normal	Inflammation and chronic bronchitis	Tuberculosis	I	II	III	LM	I	II	III	Small cell carcinoma	Other†
No. of tissue cores	63	10	13	7	30	60	68	10	3	53	8	28	110
	73		20		168				64				
No. of patients (male/female)	30 (23/7)	10 (7/3)	9 (7/2)	6 (5/1)	216 (154/62)								
	40 (30/10)		15 (12/3)										
Patient age													
Mean ± SD	49.6 ± 14.7		50.3 ± 12.5		56.9 ± 10.6								
Median	51.5		56		58								
Range	14 ~72		30 ~67		19 ~78								

Four tissue microarray slides containing individual or duplicates or triplicates of tissue cores were examined, including normal lung tissue array, lung disease spectrum tissue array, and lung cancer middensity tissue array 1 and 2. A total of 463 tissue cores obtained from 271 patients were used. For the complete list of cores and histopathological features of all samples, please visit the provider's website (www.biomax.us).
*The grades I, II, and III in pathology diagnosis are equivalent to well-differentiated, moderately differentiated, and poorly differentiated, respectively, under the microscope. I, cells appear normal and are not growing rapidly; II, cells appear slightly different from normal; III, cells appear abnormal and tend to grow and spread more aggressively. LM, lymph node metastases of squamous cell carcinoma.
†Including cores of papillary carcinoma (8), mucinous adenocarcinoma (4), bronchioloalveolar carcinoma (20), atypical and typical carcinoid (7), adenosquamous cell carcinoma (22), lung metastatic carcinoma (4), sarcoma (4), mesothelioma (2), neuroendocrine carcinoma (5), etc.

Table S2. Major proteins of interest identified by IP and LC-MS in cells transfected with Flag-Srx but not in nontransfected control cells

Proteins identified (accession ID, human)	Maximal nos. of peptides identified by LC-MS, total/unique		
	JB6, mouse	HEK293, human	A549, human
Prx I (Q06830)	3/3	12/7	8/8
Prx II (P32119)	3/2	5/5	—
Prx III (P30048)	—	3/2	12/7
Prx IV (Q13162)	6/4	70/12	21/9

Other Supporting Information Files

Dataset S1 (XLS)